Model-based strategy for grasping 3 D deformable objects using a multi-fingered robotic hand

Lazher Zaidi, Juan Antonio Corrales Ramón, Belhassen-Chedli Bouzgarrou, Youcef Mezouar, Laurent Sabourin

Model-based strategy for grasping $3D$ deformable objects using a multi-fingered robotic hand

Lazher Zaidi[a,*], Juan Antonio Corrales[b], Belhassen Chedli Bouzgarrou[b], Youcef Mezouar[b], Laurent Sabourin[b]

[a] *CESI, LINEACT Laboratory, ROUEN, FRANCE*
[b] *Universite Clermont Auvergne, CNRS, SIGMA Clermont, Institut Pascal, F-63000 Clermont-Ferrand, France.*

Abstract

This paper presents a model-based strategy for $3D$ deformable object grasping using a multi-fingered robotic hand. The developed contact model is based on two force components (normal force and tangential friction force, including slipping and sticking effects) and uses a non-linear mass-spring system to describe the object deformations due the mechanical load applied by the fingers of the robotic hand. The object-finger interaction is simulated in order to compute the required contact forces and deformations to robustly grasp objects with large deformations. Our approach is able to achieve this by using a non-linear model that outperforms current techniques that are limited to using linear models. After the contact forces computed by the simulation of the contact model guarantee the equilibrium of the grasp, they will be used as set-points for force-controlling the closing of the real fingers, and thus, the proposed grasping strategy is implemented. Two different objects (cube and sphere) made from two soft materials (foam and rubber) are tested in order to verify that the proposed model can represent their non-linear deformations and that the proposed grasp strategy can implement a robust grasp of them with a multi-fingered robotic hand equipped with tactile sensors. Thereby, both the grasping strategy and the proposed contact model are validated experimentally.

*Corresponding author
Email address: lzaidi@cesi.fr (Lazher Zaidi)

Keywords: dexterous manipulation, deformable objects, tactile sensors, multi-fingered robotic hands

1. Introduction

Robotic grasping has been studied extensively in the last two decades. Most of the research in this field has been dedicated to rigid body grasping [1] [2] [3] [4] [5] [6], and only a few studies have considered the case of deformable objects. Nevertheless, the robotised grasping of deformable objects has many potential applications in various areas, including bio-medical processing, food industry, service robotics, robotised surgery, etc [7] [8] [9].

The modelling and control of robotic hands for the grasping of $3D$ deformable objects still remains an under-researched area in the robotics community. A key issue in multi-fingered hand grasping is tracking and controlling the forces arising from the contact between the fingertips and the grasped object, so as to prevent slippage and/or excessive stresses and to ensure suitable grasp quality. When the fingers come into contact with the object, the interaction forces between the fingers and the object must be controlled. It is thus crucial to use a suitable contact model to determine the gripping forces that are necessary to impose object motion and to satisfy the friction constraints [10] [11] [12] [13] [14].

Grasping of soft objects presents two main challenges: firstly, the modelling of $3D$ soft objects with the dynamic prediction of deformations and realistic behaviour, and secondly the modelling of the interaction between a multi-fingered hand and deformable objects in order to study how such contact forces cause the deformation of the object. Indeed, the complexity of this interaction is due to the difficulty in predicting their motions, described by a high number of degrees of freedom, which makes grasp control and planning difficult. Handling deformable objects requires their deformation to be predicted using appropriate models [15] [16].

Most research in the field of robotic grasping has focused on soft-fingered

object manipulation tasks, formulating the contact constraints (normal and tangential forces) between a soft fingertip and a rigid object in $3D$ space [17] [18] [19]. However, few researchers have considered the modelling of contact interactions in the grasping and manipulation of a $3D$ deformable object. Sinha and Abel [20] introduced a model based on linear elasticity theory for soft contact regions to predict contact forces without taking into account grasp computation or the modelling of global deformation. Luo and Xiao [21] introduced an efficient model for force and deformation modeling between a rigid object and an elastic object in interactive environments. This work was extended to model the interaction between a realistic virtual human hand and an elastic object [22].

In [23][24], authors present a visually servoed deformation controller for elastic objects without estimation of the object's deformation properties. This method exploits visual feedback to iteratively estimate the deformation Jacobian matrix. This method takes into account just one contact point which cannot be used with a robotic hand for grasping and manipulation of deformable objects. Also this method is only applied to planar objects.

Grasping deformable planar objects using contact analysis was proposed in [25]. The authors proposed an algorithm to track the contact regions during the squeezing process, and determine the stick/slip mode in the contact area. In this work they presented a grasping strategy operation which squeezes the object with two fingers under specified displacements rather than forces. The finite element methods and linear elasticity theories were exploited to model object deformations, however they did not consider gravity nor the object's dynamics.

Recently, in [26], the authors propose a new approach to lift a deformable $3D$ object, causing small deformations of the object by employing two rigid fingers with contact friction. Object deformations are tracked using the finite element method (FEM) based on linear elasticity theory. The main drawback of this approach is that the grasp yields a small deformation within the scope of the linear elasticity theory and non-linear relationships between deformations and forces are not dealt with.

In [27], Mira et *al*. present a grasp planner that can reproduce the actions of a human hand to determine the contact points. Their algorithm combines the position information of the hand with visual and tactile data, to achieve a hand-object configuration in which the object is supposed to be safely grasped. This method is applied to planar object without considering the object deformation or the force applied by fingers.

In this paper, we introduce a model-based strategy for grasping $3D$ deformable objects with multi-fingered hands, by taking into account contact interactions. The grasping operation is performed with three rigid fingers on an isotropic $3D$ deformable object. Most of the approaches in the literature assume linear elastic models with small deformations and are based on classical elasticity theories, ignoring the dynamic behaviour of the object's deformation, which are unsuited for modelling large deformations. We model the object as a non-linear mass-spring system based on a tetrahedral mesh of its volume: lumped masses are attached to the nodes and non-linear springs represent the edges [28] [29]. The computation of the object's global deformation and that of the deformation of the contact areas are based on tracking of the positions of the mesh nodes by solving the dynamic motion equation based on Newton's second law. In the initial configuration, the object is assumed to be resting on a table modelled by a plane parallel to the xy plane.

The main problem addressed in real-time grasping applications is related to the stability of the friction forces and the transition between slipping and sticking modes. In section 3 of this paper, a $3D$ non-linear contact model is introduced to explain the coupling between contact forces and object deformations. In this model, the contact forces are determined with respect to the relative positions and velocities between the fingertips and the external facets of the object mesh. The fingertips of the robotic hand are approximated by hemispheres, while the manipulated object boundary surface is discretised by the triangular facets of the mesh in order to obtain an efficient implementation. This model comprises two components: a non-linear normal force [11] [12] and a non-linear tangential friction force with slipping and sticking effects. Thereby,

the contact model aims to determine the forces applied by the fingers, supposed to be rigid, on the facets of the manipulated deformable object. These forces are computed iteratively with a simulation of the contact model while closing the fingers around the object until its stability is guaranteed. These simulated contact forces are later applied as set-points for a force-controlled closing of the real fingers so that a stable grasp is implemented. The general steps of this grasping strategy are explained in section 2 and validated experimentally in section 4, in addition to the proposed contact model (which is detailed in section 3). The obtained results and the proposed contributions will be summarized in section 5.

2. GRASPING STRATEGY OF DEFORMABLE OBJECTS

As indicated in the introduction section, previous grasping strategies of deformable objects apply linear models for the relation stress-strain of the object. These models are not suitable for handling highly deformable objects since they do not give precise estimations of the contact forces generated while deforming the object. Nevertheless, a precise estimation of these forces is required not only to guarantee the static equilibrium of the object inside the robotic hand but also for avoiding applying too big forces that could damage the object.

In order to apply these optimised contact forces to the object, the grasping strategy proposed in this paper is divided into three main sequential steps (shown in the flow chart of Figure 1): 1. computation of the initial grasping configuration (green box), 2. simulation of the contact interaction fingertips-object (orange box) and 3. real execution of the fingers closing (blue box).

Thereby, the first step of the grasping strategy is to determine the initial grasp positions of the fingers over the surface of the object according to the geometrical criterion described in [29] (without considering deformations and supposing that the object lies static over a table). This initial grasp is executed in a simulation of the fingers+object system. Once the fingertips have made contact with the object, an iterative closing of the fingers is executed in this

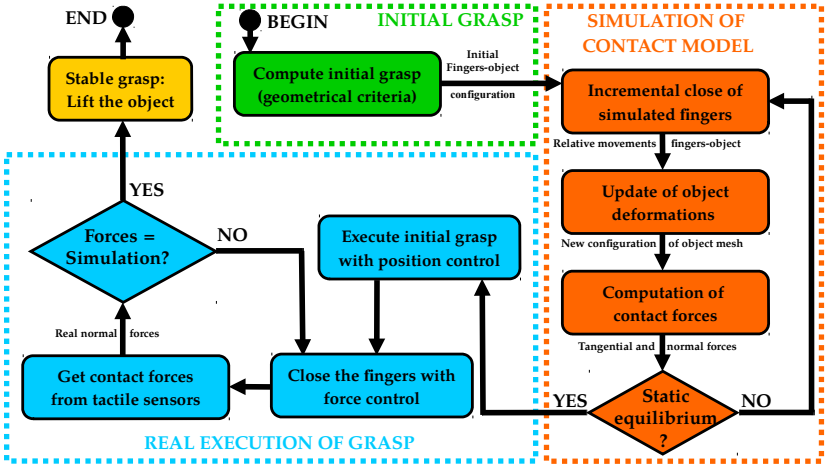

Figure 1: Flow chart of the model-based grasp strategy

simulation. The fingers are controlled in position and they perform linear movements by small increments towards the centroid of the polygon of the contact points (computed at the first step in order to get the geometrical criterion). The proposed non-linear model of the contact interaction is integrated in this simulation in order to update the deformation of the object and to compute the generated contact forces during this iterative closing process. After each simulation step (corresponding to a small displacement of the fingers towards the centroid of the contact polygon), the computed contact forces are used to evaluate the static equilibrium of the object+fingers system. The iterative process is repeated in simulation until the static equilibrium is satisfied.

After this simulation process is finished, the real grasp can be performed. Firstly, the object and the palm are installed at the same relative configuration as at the beginning of the simulation (i.e. first step). Then, the fingers are moved towards the initial contact points computed by the geometry-based grasp criterion of the first step of our strategy by applying position control. When this initial relative object-fingertips configuration is obtained, the object and the fingertips come into contact but without appreciable deformation. At this point, no more position-based control of the fingers is performed since the contact

forces have to be increased now through the deformation of the object until a stable grasp is reached (i.e. progressive squeezing of the object until it will not slide down). At this final third step, the fingers are closed by force control until the contact forces measured by the tactile sensors of their tips are equal to contact forces computed at the simulation step (i.e. second step). These contact forces guarantee the equilibrium of the object-fingertips system (as validated by the simulation). Thereby, the object can be lifted up from the table without any risk of sliding and with a minimal squeezing of its surface (i.e. minimal thresholds for contact forces). The next section will explain all the details of the non-linear model for the fingertips-object contact interactions that computes these contact force thresholds during the simulation step.

3. MODELING-SIMULATION OF CONTACT INTERACTIONS

In the second step of the grasping strategy proposed in section 2, we showed that a model of the contact interactions between the fingertips and the object is required for determining precisely the relation stress-strain during the grasping. This model will receive as input an initial grasp of the object (i.e. the initial contact points of the fingertips over the object's surface or contact polygon) without any deformation. For each incremental displacement of the fingers towards the center of the contact polygon, the deformations of the mesh representing the surface of the object are updated and the generated contact forces are computed (see Figure 1).

In order to perform this computation, the simulation of this contact model is performed in several sequential steps represented in 2. First of all, the facets of the object's mesh which are in contact with the fingertips are detected (see section 3.1). Later, contact forces are computed (section 3.3) by the evaluation of the relative velocity between the fingers and the object (section 3.2). At each iteration of the simulation, the dynamic model updates the overall shape and contact area deformations due to the applied forces (section 3.4). Finally, static equilibrium is checked for grasping stability (section 3.5).

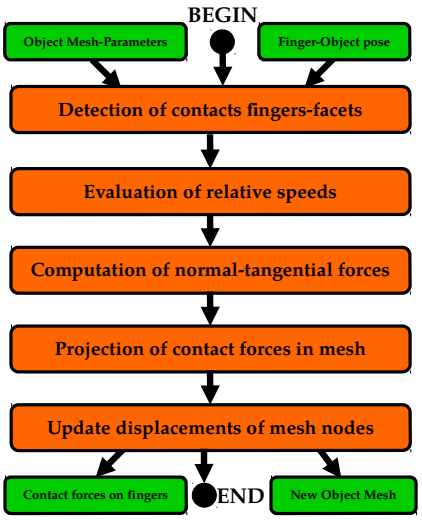

Figure 2: Flow chart of the simulation process of the non-linear model of contact interactions

This simulation scheme supposes an extension of the first version of the model presented by the authors in [29] in order to be applied in the grasping of non-linear deformable objects. In fact, not only the different mathematical components of the model at [29] are integrated in a simulation of the closing the fingers around the object but some of these mathematical components are also adapted for implementing the real grasping strategy. The next improvements are proposed:

- The new version of the model takes into account the contact of the fingertip with several facets. This enables the surface of the deformable object to conform the shape of the fingertips as precisely as the mesh density increases (see section 3.1).

- Contact forces are individually calculated for each contact point, which gives a realistic repartition of the contact pressure in the contact zone. In addition, a linear shape function has been added (see section 3.4) in order to distribute the contact forces along the mesh nodes of the surface of the object.

- The transition between sticking and slipping modes is better described in the new model by introducing two state variables u and v for each contact point to calculate the sticking forces. These two variables integrate respectively the tangential elastic displacement at the contact point and the slipping displacement which is triggered at a sticking force threshold equal to the slipping force. Both variables will be reset to zero in case of loss of contact. See section 3.3 for a complete description.

Next subsections will describe in detail all the mathematical developments for implementing these steps of the simulation of the contact model and section 4 will show how they are applied in real grasping experiments.

3.1. Contact detection

This step consists in detecting which facets of the boundary surface of the object is in contact with the fingers. The object geometry is meshed by a finite number of tetrahedral elements. Each element of the mesh has 4 nodes and 4 triangular facets. During the grasping process, any finger can be in contact with several of these triangular facets. The detection is based on the measure of the distance d_j between the center of the hemispherical fingertip $\mathbf{P}_{ci}$ and its projection point on each facet, denoted by $\mathbf{P}_{pj}$ (cf. Fig. 3). The finger and the facet are in contact when the distance, d_j is smaller than the radius of the sphere, R, and the projection of $\mathbf{P}_{pj}$ lies inside the triangle. The reference frame R_O is attached to an arbitrary fixed point O of the environment.

3.2. Computing the relative velocity between finger and facet

The velocity of the contact point $\mathbf{P}_{pj}$ related to the finger relatively to R_O is given by,

$$\mathbf{V}_{\mathbf{P}_{pj\in finger/R_O}} = \mathbf{V}_{\mathbf{P}_{ci\in finger/R_O}} + \Omega_{\mathbf{P}_{ci\in finger/R_O}} \times \mathbf{P}_{ci}\mathbf{P}_{pj} \tag{1}$$

where

$$\begin{cases} \mathbf{V}_{P_{ci\in finger/R_O}} \text{ is } 3D \text{ translational velocity of } \mathbf{P}_{ci} \\ \Omega_{P_{ci\in finger/R_O}} \text{ is } 3D \text{ rotational velocity of } \mathbf{P}_{ci} \end{cases} \tag{2}$$

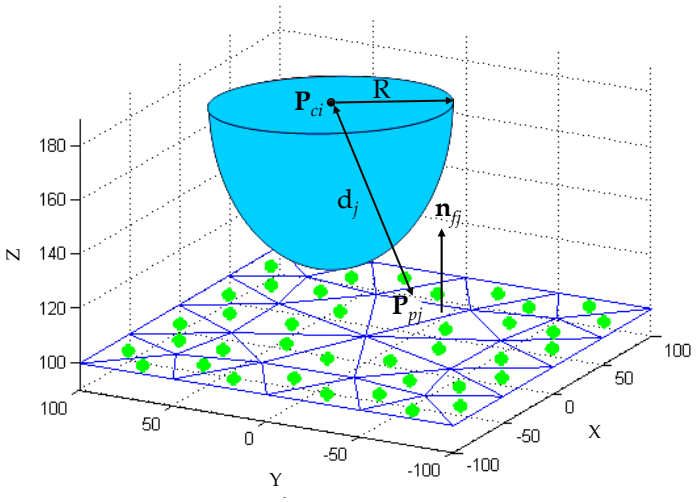

Figure 3: Contact detection

Based on the finite element interpolation method, the velocity of the contact point related to a facet is calculated by using nodal velocities of the considered facet. To this end, the area coordinates of the contact point are used (Fig. 4).

$$\mathbf{V}_{P_{pj \in facet/R_O}} = f(\mathbf{V}_{N1}, \mathbf{V}_{N2}, \mathbf{V}_{N3}) \tag{3}$$

The velocity of $\mathbf{P}_{pj}$ is determined as follows:

$$\mathbf{V}_{\mathbf{P}_{pj \in facet/R_O}} = \frac{A_1}{A_G}\mathbf{V}_{N1} + \frac{A_2}{A_G}\mathbf{V}_{N2} + \frac{A_3}{A_G}\mathbf{V}_{N3} \tag{4}$$

The relative velocity between the fingers and the facet is calculated by

$$\mathbf{V}_{rj} = \mathbf{V}_{\mathbf{P}_{pj \in finger/R_O}} - \mathbf{V}_{\mathbf{P}_{pj \in facet/R_O}} \tag{5}$$

Thereafter, the normal velocity between the finger and the facet is given by:

$$\mathbf{V}_{nj} = (\mathbf{V}_{rj} \cdot \mathbf{n}_{fj})\mathbf{n}_{fj} \tag{6}$$

The tangential velocity is then obtained by:

$$\mathbf{V}_{tj} = \mathbf{V}_{rj} - \mathbf{V}_{nj} \tag{7}$$

where

$$A_G = \sum_{i=1}^{3} A_i \tag{8}$$

where A_i $(i = 1, 2, 3)$ is the area of the triangle defined by the contact point $\mathbf{P}_{pj}$ and the facet nodes (Fig. 4).

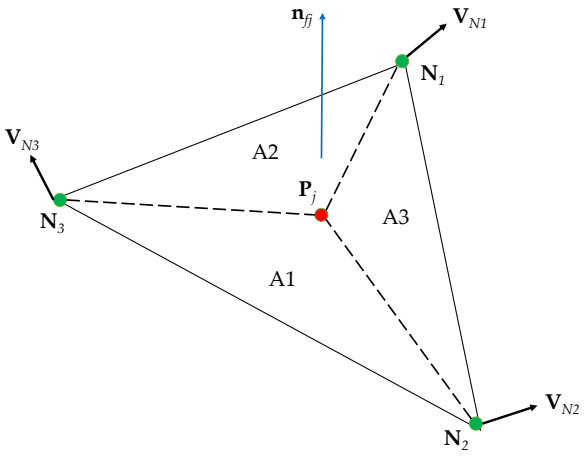

Figure 4: Interpolation of the facet nodes speeds

3.3. Contact force computation

The contact model takes into account the normal forces and the two modes of the tangential forces due to friction: slipping and sticking modes. In this model, a parallel spring - damper is attached to the ground at one end, via a slider element, and to the fingertip at the other end (Fig. 5). Therefore, the contact point location dynamically changes in the slipping condition.

In addition, we introduce two state variables, u and v, for each contact pair between the fingertips and the deformable body facets. These variables correspond to the relative displacements at the contact point due, respectively, to sticking and slipping. They are dynamically reset to zero if the contact is broken.

3.3.1. Normal force computation

Hunt and Crossley [10] have proposed a non-linear contact model to compute the normal force between a sphere and a ground. In our case, the object is modeled by a set of non-linear spring-damper pairs, then the non-linear normal force is given by,

$$f_{n_j} = \begin{cases} 0 & , \delta_j \leq 0 \\ max(0, (K\delta_j^n + C\dot{\delta_j})) \end{cases} \tag{9}$$

$$\mathbf{f}_{n_j} = f_{n_j}\mathbf{n}_{fj} \tag{10}$$

where K and C are the contact stiffness and damping constants, respectively. Based on the work presented in the literature [30], the stiffness constant is calculated by:

$$K = 2\Psi\sqrt{R} \tag{11}$$

Where Ψ is a constant calculated according to the mechanical properties of the two objects in contact, and it is given by,

$$\Psi = \frac{1}{\frac{1-v_1^2}{E_1} + \frac{1-v_2^2}{E_2}} \tag{12}$$

where E_1 and E_2 are the Young modulus, and v_1 and v_2 are the Poisson ratios of the finger and the object respectively. The damping constant is determined by,

$$C = 4\pi R\gamma \tag{13}$$

where γ is a constant.

The penetration distance δ_j is measured along the normal direction to the facet surfaces, which is defined by $\mathbf{n}_{fj}$ and is given by:

$$\delta_j = -(\mathbf{S}_{c_i}\mathbf{C}_{pj} + R\ \mathbf{n}_{fj}) \cdot \mathbf{n}_{fj} \tag{14}$$

3.3.2. Friction force computation

Grasping of a deformable object with rigid fingers is complex due to the dynamic variations of the contact region: the initial contact region deforms as the applied forces and torques vary. As a consequence of contact area deformation, the friction force can vary rapidly depending on the relative velocity and the applied load. Modeling of the tangential force, acting along each contact facet, is required in order to prevent any slippage and to ensure grasp stability. In this work, Coulomb's law is used to estimate a threshold of the transmitted tangential effort by the contact forces. This better guarantees the stability of the grasping since higher normal forces are applied if the sliding forces are underestimated. Other methods estimate the frictional force experimentally [19].

The presented model aims to predict the friction force during the grasping process. The proposed approach uses a rheological model with parallel spring-damper, in series with a slider fixing the threshold tangential force so that the contact can be estimated by Coulomb law (Fig. 5).

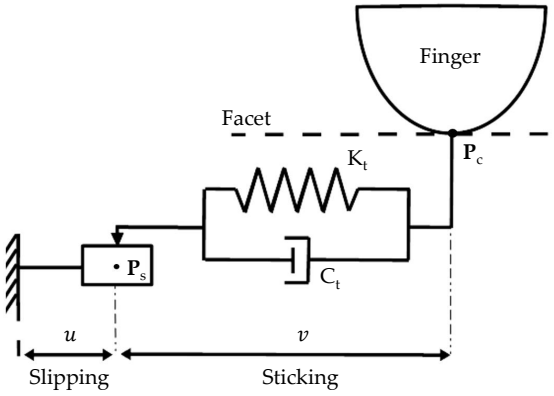

Figure 5: Friction model

The sliding friction force can be defined in terms of the Coulomb law as follow,

$$\mathbf{f}_{slip} = \begin{cases} 0 & , \|\mathbf{V}_t\| = 0 \\ -\mu f_n \frac{\mathbf{V}_t}{\|\mathbf{V}_t\|} & \end{cases} \tag{15}$$

With this model the contact point location dynamically changes in the slipping condition. If the tangential force norm is less than the threshold of sliding, then we have a sticking mode whose tangential force is defined by:

$$\mathbf{f}_{stick} = \begin{cases} 0 & , v = 0 \\ -(k_t v - c_t \dot{v}) \frac{\mathbf{P}_c\mathbf{P}_s}{\|\mathbf{P}_c\mathbf{P}_s\|} & , v > 0 \end{cases} \tag{16}$$

where v is the tangential deformation at the contact facet, $\mathbf{P}_c$ is the contact point position and $\mathbf{P}_s$ is the contact point position at the sticking regime. The parameters k_t and c_t are respectively tangential stiffness and damping coefficients estimated by using the Dopico's method [31].

The tangential force is dynamically computed by taking into account the contact surface deformations.The friction force can be expressed as shown in Algorithm 1.

In the sticking regime $\mathbf{f}_t = \mathbf{f}_{stick}$ with a deformation rate equal to the tangential velocity and zero slip speed. In the sliding case $\mathbf{f}_t = \mathbf{f}_{slip}$ with a zero deformation and a sliding speed equal to the tangential velocity.

if $\delta \leq 0$ **then**
  $f_t = 0$
else
  if $f_{stick} > \mu f_n$ **then**
    $f_t = f_{slip}$, $\dot{u} = V_t$, $\dot{v} = 0$
  else
    $f_t = f_{stick}$, $\dot{v} = V_t$, $\dot{u} = 0$
  end
end

Algorithm 1: Friction force computation

3.4. Nodal force computation

Once the generated contact forces are computed from the contact conditions for each finger, the deformations of the manipulated object can be determined.

The finger forces are expressed by means of normal and tangential components to the facet as follows:

$$\mathbf{f}_{pj} = \mathbf{f}_{n_j} + \mathbf{f}_{t_j} \tag{17}$$

The finger forces cannot be applied directly to the FEM, but we can apply nodal loads. This means that those forces must be converted into the equivalent nodal loads. The applied force $\mathbf{f}_{pj}$ must be distributed over the nodes representing facet j. The applied force is balanced by the sum of the reaction forces $\mathbf{f}_l$ $(l = 1, 2, 3)$ from the nodes of the facet (Fig. 6). The local equilibrium force condition can therefore be written as:

$$\mathbf{f}_{pj} = \sum_{l=1}^{3} \mathbf{f}_l \tag{18}$$

Linear shape functions are used to compute the equivalent nodal distribution of the contact forces [32]. The nodal forces are then calculated using the matrix shape function $\mathbf{H}$, based on the area coordinates of the facet contact point (Fig. 6).

$$\mathbf{H} = \begin{bmatrix} \frac{A_1}{A_G} & 0 & 0 & \frac{A_2}{A_G} & 0 & 0 & \frac{A_3}{A_G} & 0 & 0 \\ 0 & \frac{A_1}{A_G} & 0 & 0 & \frac{A_2}{A_G} & 0 & 0 & \frac{A_3}{A_G} & 0 \\ 0 & 0 & \frac{A_1}{A_G} & 0 & 0 & \frac{A_2}{A_G} & 0 & 0 & \frac{A_3}{A_G} \end{bmatrix}$$

The node forces are then computed using the Eq. (19).

$$\mathbf{H}^T \mathbf{f}_{pj} = \mathbf{f}_l \tag{19}$$

$$with\ \mathbf{f}_l = \begin{bmatrix} f_1x\ f_1y\ f_1z\ f_2x\ f_2y\ f_2z\ f_3x\ f_3y\ f_3z \end{bmatrix}'_{R_O} \tag{20}$$

3.5. Static equilibrium

After computing the normal and tangential forces at each contact, it is possible to satisfy the required conditions for static equilibrium. In order to pick up the object, the resulting vertical force generated by the three fingers must balance the object's weight w.

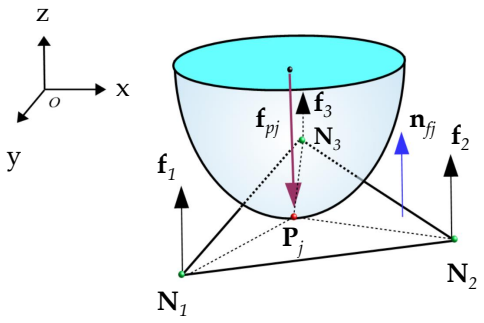

Figure 6: Nodal forces from finger contact forces

We suppose that the external forces, named $\mathbf{f}_w$, result only from the gravity effect acting in the negative Z direction of the reference frame R_0 .The equilibrium equations can then be written as:

$$\sum_{j=1}^{n}(\mathbf{f}_{n_j}) + \sum_{j=1}^{n}(\mathbf{f}_{t_j}) + \mathbf{f}_w = \mathbf{0} \tag{21}$$

$$\sum_{j=1}^{n}(\mathbf{f}_{n_j} \times \mathbf{C}_{j_O}) + \sum_{j=1}^{n}(\mathbf{f}_{t_j} \times \mathbf{C}_{j_O}) + \mathbf{f}_w \times \mathbf{C}_{G_O} = \mathbf{0} \tag{22}$$

where $\mathbf{C}_{j_O}$ represents the position vector from the contact point at the facet j to the reference frame R_O origin O. $\mathbf{C}_{G_O}$ is the position vector from the object mass center G to the reference frame R_O origin O.

4. EXPERIMENTAL RESULTS

The non-linear contact model described in section 3 and its application to the proposed grasping strategy of section 2 are validated with several real experiments with a multi-fingered robotic hand grasping different deformable objects. Section 4.1 describes the robotic platform and section 4.2 presents the two deformable objects (cube and sphere) with two different materials (foam and rubber, respectively) that are used in the experiments. Section 4.2 also details the compression tests that are performed not only to characterize the

mechanical parameters of the two materials (i.e. Young's modulus and Poisson's ratio) required by the model but also to justify the non-linearity of the strain-stress relations of the soft materials. Finally, section 4.3 presents the experiments done for validating the contact model firstly (by touching the cube with one finger and verifying that the real relation deformation-force matches the relation computed by the simulation of the contact model) and the grasping strategy later (by grasping the sphere with three fingers of the robotic hand). Section 5 will present a global analysis of the results of these experiments.

4.1. Robotic platform

The robotic platform used to validate the results of this paper is composed by two Kuka LWR4+ arms and a Shadow hand installed at the end-effector of one of these arms (Fig. 7).

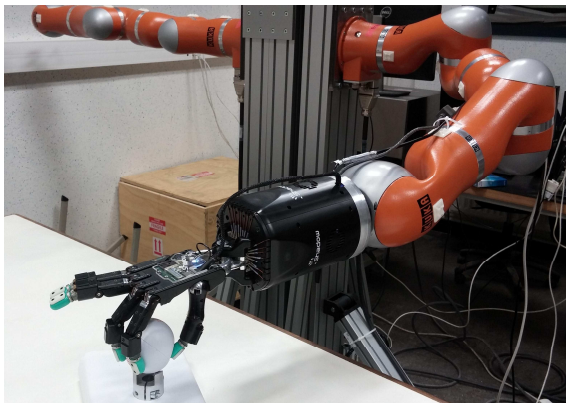

Figure 7: Robotic platform

Both arms have 7 DOF in order to be redundant for manipulation in cluttered environments while the hand contains 19 DOF so that complex in-hand manipulation tasks can be executed. Each of the fingers of the hand is equipped at its tip with a BioTac tactile sensor. These biomimetic tactile sensors provide not only normal forces applied over the surface of the sensor in a matrix of electrodes, but also vibrations-texture and temperature for a complete char-

acterization of the contact. In our experiments, we have extracted the total contact force applied on each fingertip from these tactile sensors.

4.2. The deformable objects

In order to calibrate our simulation models, the values of the mechanical parameters of the objects to be grasped should be identified, namely, the Young's modulus and the Poisson's ratios.

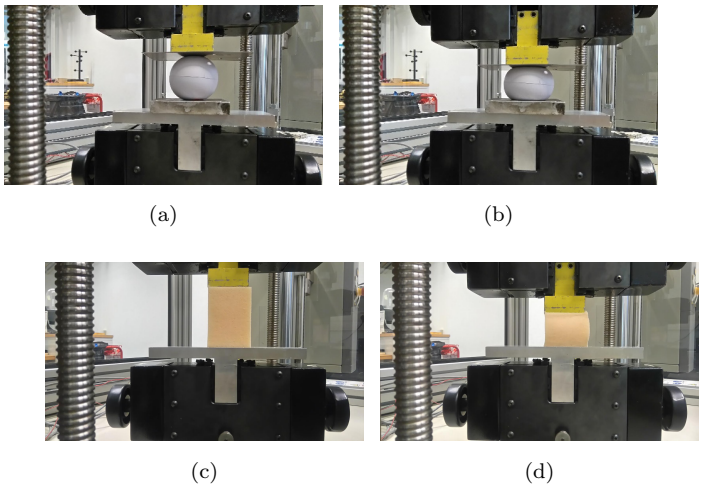

(a) (b)

(c) (d)

Figure 8: Compression tests applied to (a)-(b) a soft sphere of rubber and (c)-(d) a soft cube of foam

For this, we performed compression tests in the longitudinal direction on objects that will be used in our grasping tasks. As an example, we present here the test effected to a significantly deformable soft sphere with a radius of 0.064 m and a mass of 0.05 Kg (Section 4.3.3).

The curve presented in Figure 9 gives the stress evolution according to compressive deformation, from which its Young's modulus and Poisson's ratios are obtained by applying the method indicated in [33]. The elasticity parameters of both objects are listed in Table 1.

The same method is applied to the cube that will be used in section 4.3.1. The objects are modeled by a tetrahedral mesh obtained from ANSYS while the

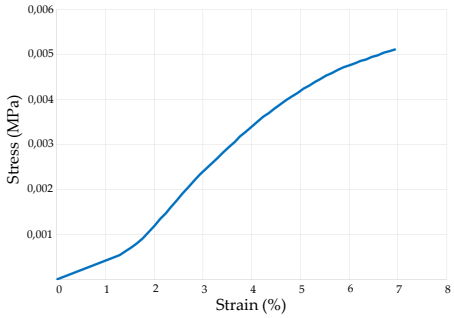

Figure 9: Stress evolution according to compressive deformation

Table 1: Mechanical parameters used for object model calibration and contact force determination

	Cube	Sphere
Young's modulus (MPa)	4,9284	0,0793
Poisson's ratios	0.39	0.45

resolution of the dynamic differential equations is performed in Matlab using an explicit Runge - Kutta formula [29].

4.3. Experimental evaluation

An experimental evaluation is performed in order to validate the proposed contact model by executing a real grasping task.

4.3.1. Validation of the contact model

In order to validate the proposed model of contact, it is necessary to compare the computed forces in simulation with the measured ones in the real task. Figure 10 shows the interaction of the finger with a deformable cube in simulation and in experimental.

The $3D$ graphical representation of the hand, is implemented using Matlab Toolbox Syngrasp [34] (shown in Fig. 10).

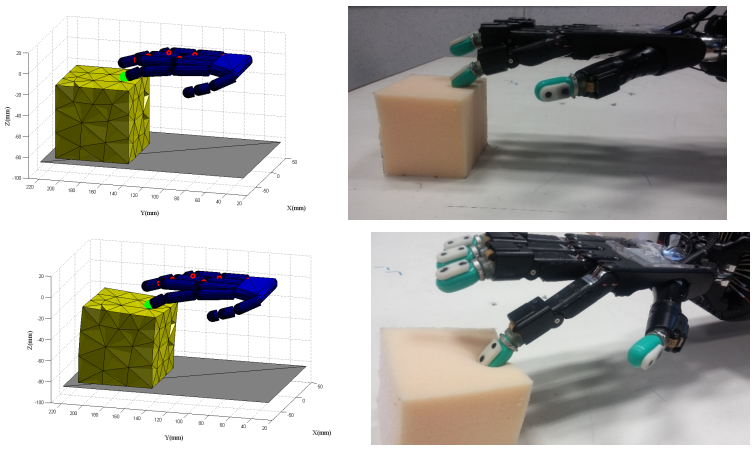

Figure 10: Validation of the contact model

The relation between the applied force and the penetration (deformation) is depicted in Figure 11. We see from this figure that the proposed interaction model gives results consistent with the results obtained experimentally. In fact, the mean error of the contact force obtained by our model is of $0.3N$, which implies only a 15% of typical contact forces required for grasping most common life deformable object. In addition, the non-linear relation penetration-force shows that simplified linear models cannot be used for grasping significantly deformable objects and justifies the necessity of the proposed model.

4.3.2. Simulation results

As indicated in the flowchart presented in Figure 1, the first step of the grasping strategy is to position the fingers over the surface of the object at the points established by the geometric criterion (see [35] [36] [37] for more details). This criterion ensures force-closure grasps. An iterative simulation of the proposed interaction contact model is executed. At each iteration of this simulation, all fingers are moved synchronously towards the centroid of the grasping triangle from the geometric criterion (see Fig. 12) by applying a Cartesian control based on the $WDLS$ (Weighted Damped Least-Squares) method [38]. After this movement, deformations and contact forces are computed by the proposed

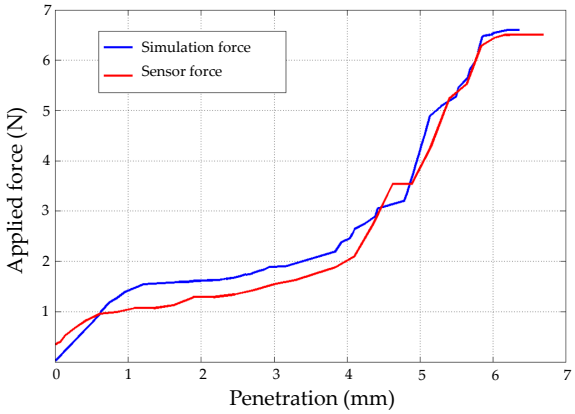

Figure 11: Evaluation of the applied force with regard to the penetration

contact model. When grasp stability is achieved, the simulation stops and the final contact forces are returned as result.

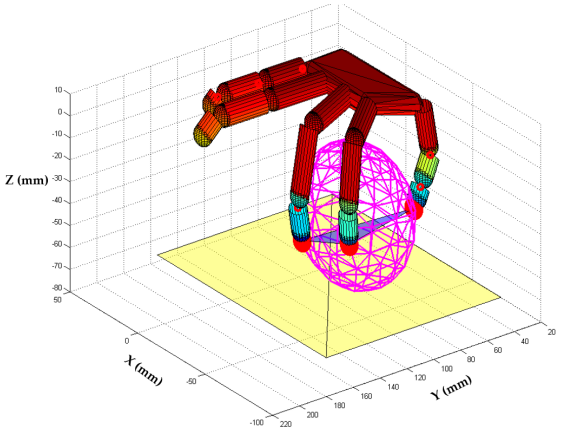

Figure 12: Force closure grasp of the sphere

At each iteration the dynamic system update the resulting deformations from the applied forces. In order to maintain the object during the handling operation, the applied forces must satisfy the constraints given by equations (21) and (22). The evaluation of the applied forces is ensured by the tracking

of their norm.

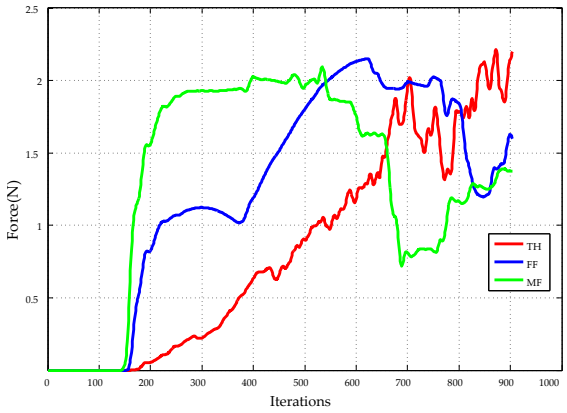

Figure 13: Grasping forces applied by the three fingers

Figure 13 shows the variation in the norm of the three forces applied to the object. At the initial step the fingers start to move toward the object. When the fingers come in contact with the object, the contact model starts to evaluate the applied forces. This figure also shows that the contact forces are continuous and directly related to the amount of local deformation inside the contact area. The fingers continue to apply forces until equilibrium conditions are satisfied. Once this state is reached, the fingers maintain the forces applied to the object in order to ensure stable handling.

Table 2 shows the penetration depth of each finger measured from the initial contact and the final position of each finger.The forces ensuring the grasp equilibrium are also presented.

4.3.3. Planning of a grasping operation

The contact forces obtained from the previous simulation process are used as desired values for performing a force-based control of the real fingers based on the measurements of the tactile sensors installed at their tips. Figure 14 shows the matching between the real experiment and simulation.

The relation between the penetration of each finger into the surface of the

Table 2: Grasping parameters

	Penetration depth (mm)	Forces (N)
Thumb	20	2.2
First finger	15	1.6
Middle finger	12	1.3

sphere and the contact force is shown in Figure 15.

The grasping operation is built according to several criteria such as force limit to be respected by fingers, contact forces positions and forces directions [37]. During grasping operations, system configuration has to remain in force closure grasp conditions along fingertips trajectories while squeezing the deformable object. To this end, the trajectory generation we have used consists in straight line movements of the fingertips from the initial contact points to the grasp plane center. This enables the three fingers to reach the contact force thresholds in stable grasp conditions. In addition, the thumb has to generate a larger deformation and exert a greater force in order to balance the opposite forces of the first and middle fingers.

5. CONCLUSIONS AND RESULTS ANALYSIS

An approach for modeling the interactions between deformable objects and a robotic hand has been presented. This approach overcomes the limitations of previous works that do not consider large deformations of the grasp object, where either a linear behaviour is assumed or the contact's evolution is ignored. The proposed model comprises two components: a non-linear normal force and a non-linear tangential friction force with slipping and sticking effects. With this model, deformable objects with non-linearities in the penetration-force relation can be actually grasped and lifted without any slipping. This model can be used to characterize the deformation of the grasped object according to the contact forces. In addition, the interactions between the fingers and the object

can be simulated in order to plan real grasping tasks of significantly deformable objects. In fact, this paper proposes a new algorithm to perform this interaction simulation and then estimate the contact forces that are required to analyse the grasp stability and update object deformations. The contact forces computed by the simulation of the model will be used as set-points for a real force-controlled closing of the fingers. Previous grasping strategies computing stability from force measurements of tactile sensors will not be so precise as the proposed approach since these sensors only consider normal forces but not tangential ones.

The proposed grasping strategy has been successfully tested in the execution of stable grasps of very soft objects (i.e. a rubber sphere and a foam cube) with a multi-fingered robotic hand. The cube was used to validate with a real experiment the validity of the new contact model and its ability to represent non-linear stress-strain relations: Figure 9 shows the real data of the sphere obtained from compression tests and Figure 11 compares the real data of the cube from the data computed by the simulation of the contact model. As Figure 11 shows, the real relation force-penetration is very similar to the one computed in the simulation and shows the suitability of applying the contact forces obtained from the simulation to perform a real grasping strategy of the object.

Finally, the other object (i.e. the sphere) is used to test in a real experiment the new grasping strategy proposed in the paper and based in the contact model. This experiment validates again the non-linearity of the force-penetration relation (Figure 15), which justifies the necessity of taking into account the proposed contact model in order to get a precise estimate of the contact forces generated by a deformation of the surface of the object produced by the fingertips. These contact forces computed from the contact model while simulating the closing of the fingertips (see Figure 13 and their values in Table 2) are later used as set-points in order to close the real fingers with force control and guarantee a stable grasp of the object (i.e. keeping the object in equilibrium inside the hand without sliding if the hand lifts up the object). Since the contact forces

are computed incrementally during the closing of the fingers until equilibrium is reached, the final contact forces obtained from simulation are minimal and the corresponding deformation of the object could not be too important. For instance, in the proposed experiment, the performed deformation is much more visible in the thumb (Figures 14(e)-(f)). This behaviour will guarantee that the object is not damaged by applying unnecessarily too high contact forces.

In future work, the authors will extend the proposed model-based strategy in order to obtain a dexterous manipulation planner where the deformable object will not only be restrained by the fingers but also moved and reoriented inside the robotic hand.

ACKNOWLEDGMENTS

This work is sponsored by the French government research program "Investissements d'avenir" through the RobotEx Equipment of Excellence (ANR-10-EQPX-44), by the European Union through the Regional Competitiveness and Employment Program 2007-2013 (ERDF - Auvergne region), by the SIGMA Clermont Engineering School and by the Auvergne regional council.

References

[1] A. Bicchi, V. Kumar, Robotic grasping and contact: a review, in: Robotics and Automation, 2000. Proceedings. ICRA '00. IEEE International Conference on, Vol. 1, 2000, pp. 348–353 vol.1. doi:10.1109/ROBOT.2000.844081.

[2] M. A. Roa, R. Suarez, Computation of independent contact regions for grasping 3-d objects, IEEE Transactions on Robotics 25 (4) (2009) 839–850. doi:10.1109/TRO.2009.2020351.

[3] Y. Lin, Y. Sun, Robot grasp planning based on demonstrated grasp strategies, The International Journal of Robotics Research (2014) 0278364914555544.

[4] A. Miller, P. K. Allen, Graspit!: A versatile simulator for robotic grasping, IEEE Robotics and Automation Magazine 11 (4) (2004) 110–122. doi:10.1109/MRA.2004.1371616.

[5] A. Bernardino, M. Henriques, N. Hendrich, J. Zhang, Precision grasp synergies for dexterous robotic hands, in: 2013 IEEE International Conference on Robotics and Biomimetics (ROBIO), 2013, pp. 62–67. doi:10.1109/ROBIO.2013.6739436.

[6] D. Flavigne, V. Perdereau, A learning-free method for anthropomorphic grasping, in: 2013 IEEE/RSJ International Conference on Intelligent Robots and Systems, 2013, pp. 2985–2990. doi:10.1109/IROS.2013.6696779.

[7] R. Jansen, K. Hauser, N. Chentanez, F. van der Stappen, K. Goldberg, Surgical retraction of non-uniform deformable layers of tissue: 2d robot grasping and path planning, in: Intelligent Robots and Systems, 2009. IROS 2009. IEEE/RSJ International Conference on, 2009, pp. 4092–4097. doi:10.1109/IROS.2009.5354075.

[8] A. Ohev-Zion, A. Shapiro, Towards Autonomous Robotic Systems: 12th Annual Conference, TAROS 2011, Sheffield, UK, August 31 – September 2, 2011. Proceedings, Springer Berlin Heidelberg, Berlin, Heidelberg, 2011, Ch. Grasping of Deformable Objects Applied to Organic Produce, pp. 396–397.

[9] M. C. Gemici, A. Saxena, Learning haptic representation for manipulating deformable food objects, in: Intelligent Robots and Systems (IROS 2014), 2014 IEEE/RSJ International Conference on, 2014, pp. 638–645. doi:10.1109/IROS.2014.6942626.

[10] K. Hunt, F. Crossley, Coefficient of restitution interpreted as damping in vibroimpact, Journal of applied mechanics 42 (2) (1975) 440–445.

[11] N. Xydas, I. Kao, Modeling of contact mechanics and friction limit surfaces for soft fingers in robotics, with experimental results, The International Journal of Robotics Research 18 (9) (1999) 941–950.

[12] Y. Gonthier, J. McPhee, C. Lange, J.-C. Piedboeuf, A regularized contact model with asymmetric damping and dwell-time dependent friction, Multibody System Dynamics 11 (3) (2004) 209–233.

[13] P. Flores, M. Machado, M. T. Silva, J. M. Martins, On the continuous contact force models for soft materials in multibody dynamics, Multibody System Dynamics 25 (3) (2010) 357–375.

[14] R. Featherstone, Rigid body dynamics algorithms, Springer, 2014.

[15] S. F. Gibson, B. Mirtich, A survey of deformable modeling in computer graphics, Tech. rep., Citeseer (1997).

[16] J. Wu, R. Westermann, C. Dick, A survey of physically based simulation of cuts in deformable bodies, in: Computer Graphics Forum, Vol. 34, 2015, pp. 161–187.

[17] M. Ciocarlie, C. Lackner, P. Allen, Soft finger model with adaptive contact geometry for grasping and manipulation tasks, in: EuroHaptics Conference, 2007 and Symposium on Haptic Interfaces for Virtual Environment and Teleoperator Systems. World Haptics 2007. Second Joint, IEEE, 2007, pp. 219–224.

[18] T. Inoue, S. Hirai, Parallel-distributed model in three-dimensional soft-fingered grasping and manipulation, in: Robotics and Automation, 2009. ICRA'09. IEEE International Conference on, IEEE, 2009, pp. 2092–2097.

[19] T. Watanabe, Y. Fujihira, Experimental investigation of effect of fingertip stiffness on friction while grasping an object, in: Robotics and Automation (ICRA), 2014 IEEE International Conference on, 2014, pp. 889–894. doi:10.1109/ICRA.2014.6906959.

[20] P. R. Sinha, J. Abel, A contact stress model for multifingered grasps of rough objects, Robotics and Automation, IEEE Transactions on 8 (1) (1992) 7–22.

[21] Q. Luo, J. Xiao, Contact and deformation modeling for interactive environments, Robotics, IEEE Transactions on 23 (3) (2007) 416–430. doi:10.1109/TRO.2007.895058.

[22] T. Cui, J. Xiao, A. Song, Simulation of grasping deformable objects with a virtual human hand, in: Intelligent Robots and Systems, 2008. IROS 2008. IEEE/RSJ International Conference on, 2008, pp. 3965–3970. doi:10.1109/IROS.2008.4651080.

[23] D. Berenson, Manipulation of deformable objects without modeling and simulating deformation, in: Intelligent Robots and Systems (IROS), 2013 IEEE/RSJ International Conference on, 2013, pp. 4525–4532. doi:10.1109/IROS.2013.6697007.

[24] D. Navarro-Alarcon, Y. Liu, J. G. Romero, P. Li, Visually servoed deformation control by robot manipulators, in: Robotics and Automation (ICRA), 2013 IEEE International Conference on, 2013, pp. 5259–5264. doi:10.1109/ICRA.2013.6631329.

[25] Y. Jia, F. Guo, H. Lin, Grasping deformable planar objects: Squeeze, stick/slip analysis, and energy-based optimalities, I. J. Robotic Res. 33 (6) (2014) 866–897.

[26] H. Lin, F. Guo, F. Wang, Y.-B. Jia, Picking up a soft 3d object by feeling the grip, The International Journal of Robotics Research-doi:10.1177/0278364914564232.

[27] D. Mira, A. Delgado, C. M. Mateo, S. T. Puente, F. A. Candelas, F. Torres, Study of dexterous robotic grasping for deformable objects manipulation, in: Control and Automation (MED), 2015 23th Mediterranean Conference on, 2015, pp. 262–266. doi:10.1109/MED.2015.7158760.

[28] E. Nabil, B. Belhassen-Chedli, G. Grigore, Soft material modeling for robotic task formulation and control in the muscle separation process, Robotics and Computer-Integrated Manufacturing 32 (2015) 37–53.

[29] L. Zaidi, B.-C. Bouzgarrou, L. Sabourin, Y. Mezouar, Modeling and analysis of 3d deformable object grasping, in: Robotics in Alpe-Adria-Danube Region (RAAD), 2014 23rd International Conference on, 2014, pp. 1–8.

[30] K. L. Johnson, Contact mechanics, Cambridge University Press, 1987.

[31] D. Dopico, A. Luaces, M. Gonzalez, J. Cuadrado, Dealing with multiple contacts in a human-in-the-loop application, Multibody System Dynamics 25 (2) (2011) 167–183.

[32] H. Ahmadian, S. Farughi, Shape functions of superconvergent finite element models, Thin-Walled Structures 49 (9) (2011) 1178–1183.

[33] R. Verrall, A sphere compression test for measuring the mechanical properties of dental composite materials, Journal of Dentistry 4 (1) (1976) 11 – 14.

[34] M. Malvezzi, G. Gioioso, G. Salvietti, D. Prattichizzo, A. Bicchi, Syngrasp: A matlab toolbox for grasp analysis of human and robotic hands, in: Robotics and Automation (ICRA), 2013 IEEE International Conference on, 2013, pp. 1088–1093. doi:10.1109/ICRA.2013.6630708.

[35] N. Daoud, J. Gazeau, S. Zeghloul, M. Arsicault, A real-time strategy for dexterous manipulation: Fingertips motion planning, force sensing and grasp stability, Robotics and Autonomous Systems 60 (3) (2012) 377 – 386.

[36] L. Zaidi, B. Bouzgarrou, J. Corrales, Y. Mezouar, L. Sabourin, Stable grasping of soft objects based on a 3d deformation model with visual and tactile feedback, in: IROS workshop on multimodal sensor-based robot control for HRI and soft manipulation, Hamburg, Allemagne, 2015.

[37] L. Zaidi, B.-C. Bouzgarrou, J. Corrales, Y. Mezouar, L. Sabourin, Interaction modeling in the grasping and manipulation of 3d deformable objects, in: Advanced Robotics (ICAR), 2015 International Conference on, 2015, pp. 504–509.

[38] S. Chiaverini, B. Siciliano, O. Egeland, Review of the damped least-squares inverse kinematics with experiments on an industrial robot manipulator, IEEE Transactions on Control Systems Technology 2 (2) (1994) 123–134. doi:10.1109/87.294335.

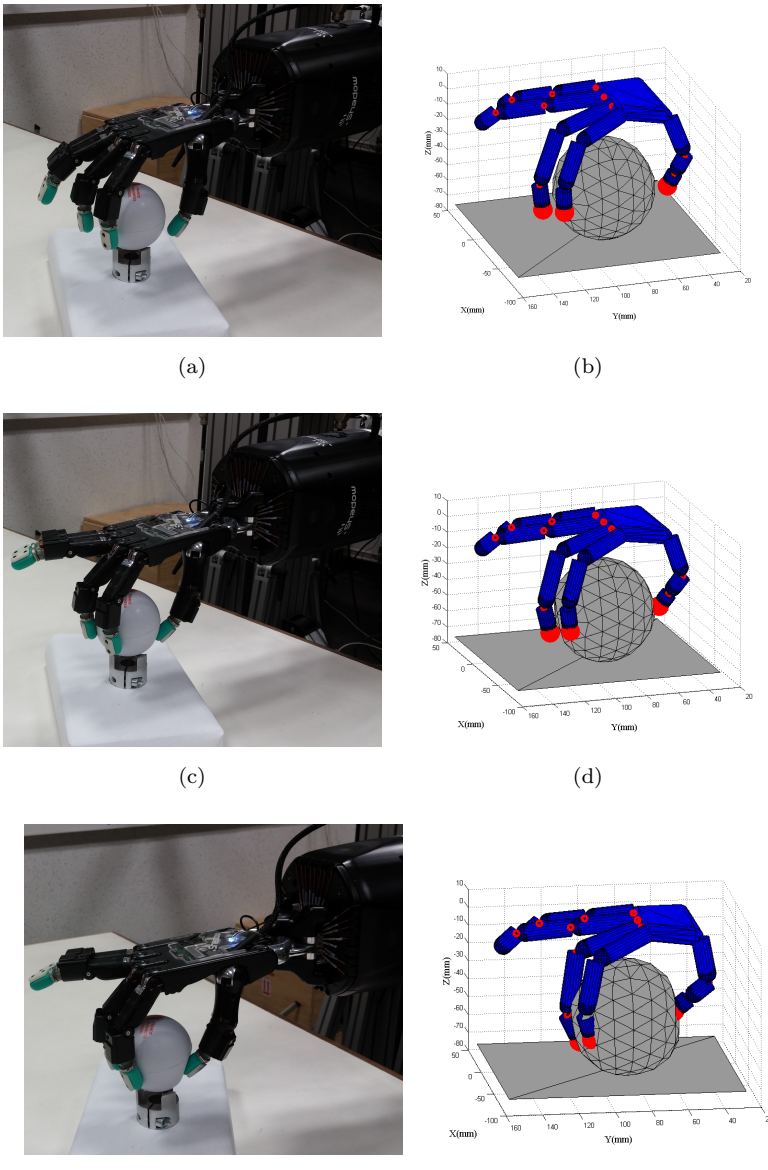

(a) (b)

(c) (d)

(e) (f)

Figure 14: Frames (real and simulation) of a grasp task: (a)-(b) Initial grasping pose, (c)-(d) Initial contact, (e)-(f) Final object deformations from applied forces

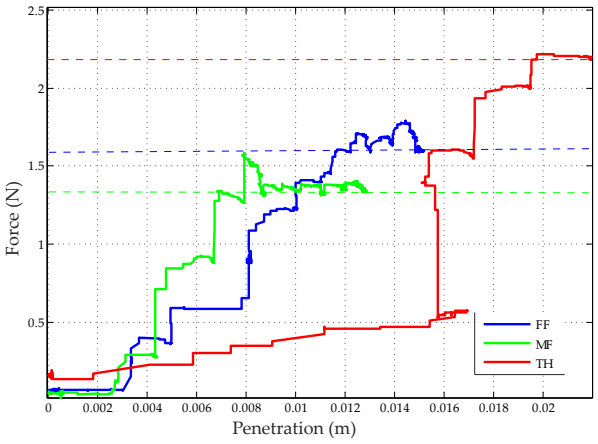

Figure 15: Grasping forces applied by the shadow fingers